

## Coherent control of molecular modulation

S. N. Goda,<sup>a)</sup> S. Sensarn, M. Y. Shverdin,<sup>b)</sup> and G. Y. Yin  
Edward L. Ginzton Laboratory, Stanford University, Stanford, California 94305, USA

(Received 31 July 2007; accepted 17 September 2007; published online 10 December 2007)

We demonstrate coherent control of a molecular modulation process using an incident set of seven optical sidebands spanning two octaves of bandwidth. We utilize a genetic algorithm to optimize the relative phases of the incident sidebands to generate additional UV sidebands with nearly 1% efficiency, change the ratio of energy between sidebands by more than a factor of 50, and efficiently alter individual sideband energies by millijoules. © 2007 American Institute of Physics.  
[DOI: 10.1063/1.2821382]

A common method for achieving molecular modulation or the adiabatic excitation of a molecular transition is to use two lasers whose frequency difference is slightly detuned from Raman resonance.<sup>1,2</sup> The driven molecular motion modulates the two driving lasers causing the generation of a set of coherent sidebands of Bessel function spectral amplitudes with near unity overall efficiency. With sufficiently intense laser beams, the molecular coherence can be large enough that the generation length and phase-slip length become nearly equal resulting in all sidebands being collinear as well. The use of molecular modulation for ultrashort pulse generation has been studied for nearly a decade.<sup>2</sup> Initially, the fundamental vibrational transition in deuterium ( $D_2$ ) gas was used to generate four octaves of bandwidth.<sup>3</sup> Variations evolved including using the rotational transition in  $H_2$  (Ref. 4), multiplicative and additive techniques allowing the generation of hundreds of sidebands,<sup>2,5</sup> modulation of  $\sim 100$  fs pulses as a first step toward generating single, energetic ultrashort pulses,<sup>6</sup> as well as generation within a hollow fiber allowing the use of less energetic source lasers.<sup>7</sup>

In this letter, we report experiments toward prescribed multioctave spectrum generation using coherent control of molecular modulation. We use a set of seven sidebands totaling  $\sim 10$  mJ of energy, originally generated through molecular modulation in  $D_2$  gas, to drive molecular modulation in a second  $D_2$  chamber. Each consecutive pair within the seven frequencies is naturally tuned close to the Raman resonance allowing the magnitude of the molecular coherence and efficiency of the mixing process to be controlled by adjusting the relative phases of the seven sidebands. An evolutionary algorithm optimizes these phases to generate additional UV sidebands with nearly 1% efficiency, change the ratio of energy between sidebands by more than a factor of 50, and efficiently alter individual sideband energies by millijoules.

Of particular relevance to this letter, a first experiment using three sidebands to explore the effect of relative sideband phasing on molecular coherence excitation has been performed.<sup>8</sup> In addition, there is a body of prior work in the shaping of femtosecond scale pulses by evolutionary algorithms to control nonlinear-optical processes. Control has been shown over high-order harmonic spectra generation,<sup>9</sup>

Raman mode excitation in a molecule,<sup>10</sup> and spatial location of laser-induced breakdown.<sup>11</sup>

Figure 1 depicts the experimental setup. The experimental details for the generation of the initial seven sidebands are the same as previous work<sup>12</sup> and are described here only briefly. We use two  $Q$ -switched lasers tuned 300 MHz below Raman resonance to adiabatically excite the fundamental vibrational transition in 50 torr of  $D_2$  gas cooled to 77 K. A discrete set of frequency components separated by  $2994\text{ cm}^{-1}$  and spanning nearly four octaves of bandwidth is generated under an envelope of 12 ns. A seven sideband subset is dispersed, passed through a Jenoptik liquid-crystal spatial light modulator, recombined, and recollimated. The subset has wavelengths of 1563, 1064, 807, 650, 544, 468, and 410 nm. These seven components are focused with a 40 cm achromatic lens into a 30 cm long target chamber filled with 200 torr of  $D_2$  gas cooled with liquid nitrogen to 77 K. The confocal parameters within the chamber range from 2 cm to 5 cm and the Raman detuning in the second cell is 500 MHz below resonance. The choice of 40 cm focal length for the lens and 200 torr pressure for the target chamber are both experimentally determined to maximize generation of new sidebands. Numerical simulations (based upon eigenvector solutions from previous theory<sup>1</sup>) predict a maximum coherence of  $\rho \approx 0.25$  in the target chamber under these conditions. Although the simulations qualitatively showed ability to control sideband energies and ratios through phase control of the incident seven sidebands, quantitatively they predicted more efficient generation of new UV sidebands than observed.

After the target cell, three additional generated ultraviolet sidebands (with wavelengths 365, 330, and 300 nm) ex-

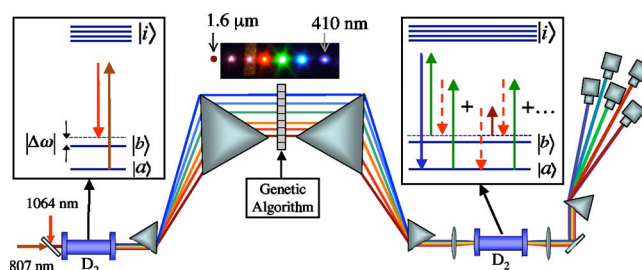


FIG. 1. (Color online) Experimental setup. Seven Raman sidebands are generated in a  $D_2$  cell. They are dispersed, passed through a spatial light modulator, recombined, recollimated, and focused into a target  $D_2$  chamber. The resultant sideband spectrum generated through four-wave Raman mixing is measured by an array of photodiodes.

<sup>a)</sup>Electronic mail: sngoda@gmail.com.

<sup>b)</sup>Present address: Lawrence Livermore National Laboratory, Livermore, CA 94550, USA.

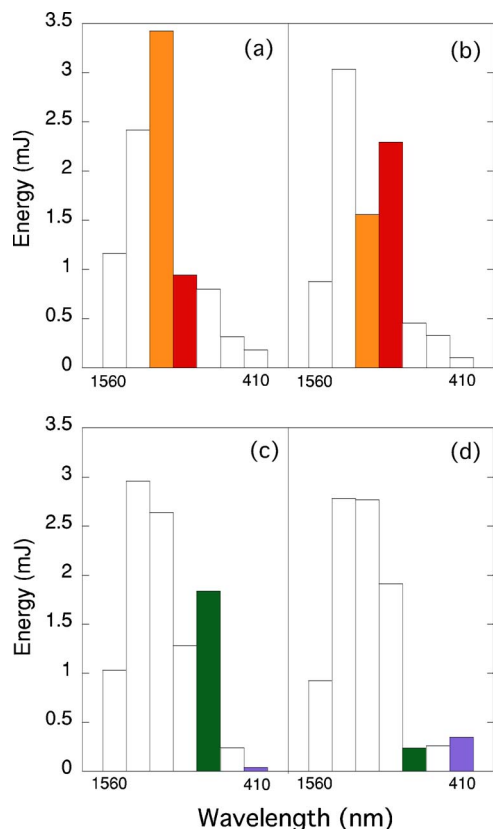


FIG. 2. (Color online) Maximizing and minimizing the ratio of sideband energies. Each subfigure depicts the energies of seven sidebands after an optimization, with the two wavelengths being optimized shown in solid. In part (a), the energy ratio of the 807 nm sideband to the 650 nm sideband is maximized to 3.6. Part (b) shows minimization of the same ratio to 0.68. In part (c), the energy ratio of the 544 nm sideband to the 410 nm sideband is maximized to 48. Part (d) shows minimization of the same ratio to 0.67.

tend the original frequency comb from seven to ten sidebands. We collimate all sidebands with a 30 cm achromatic lens and split them into two beams with a UV beamsplitter. The original seven sidebands are dispersed with an SF10 prism while the three UV sidebands are dispersed with a fused-silica prism. An array of laboratory-built photodiodes with sufficient bandwidth to resolve the 12 ns  $Q$ -switched structure of each sideband measures the intensity profile of all ten sidebands simultaneously. These photodiode signals are sent to boxcar integrators (SRS SR250) that in turn pass the integrated photodiode signals to a computer through a data acquisition board (NI PCI-1200). Since we possess only two boxcar integrators, the photodiode signals are sent through a laboratory-built analog multiplexer which passes any two signals at one time to the integrators. A computer program selects which photodiode signals are passed by the multiplexers and, by cycling the selection, serially passes all photodiode signals to the boxcar integrators. Absolute energies are measured by calibrating the integrated photodiode signals with energy measurements from a calibrated pyroelectric sensor (Coherent Moletron J4-09).

For the experiments described below, we use a genetic algorithm (GA) to adjust the relative phases of the original seven sidebands or, equivalently, the incident pulse shape by controlling the voltages applied to the liquid crystal spatial light modulator. The GA begins by randomly picking sets of phases and measuring a prescribed fitness function (representing the quality to be optimized) for each pulse shape.

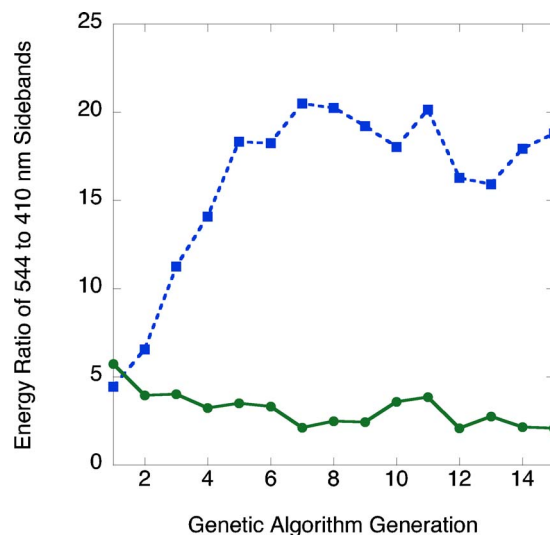


FIG. 3. (Color online) Convergence of the GA during an optimization of the ratio of 544 nm energy to 410 nm energy. Each point represents the average energy ratio over the ten different pulse shapes of one generation of the GA. Values for the minimization of the energy ratio are depicted by circles connected by a solid line and values for maximization of the ratio are depicted by squares connected by a dotted line.

The GA uses an evolutionary strategy to create the next generation of pulse shapes by breeding the best performing pulse shapes from the previous generation and sometimes introducing random mutations. After a number of generations, the GA should converge to a set of phases which optimizes the fitness function.<sup>13</sup>

In order to maximize generation of extra UV sidebands, we choose as our fitness function the integrated photodiode signal from the first UV sideband since it is the most energetic. The GA uses ten pulse shapes per generation and executes for five generations for an optimization. Using a sum incident energy of 10.6 mJ ( $\pm 10\%$  from pulse to pulse), we were able to achieve a total UV conversion efficiency of 1.3% with efficiencies of 0.8%, 0.4%, and 0.08% for wavelengths of 365, 330, and 300 nm, respectively. This efficiency of conversion into the UV closely matches previously reported results.<sup>3</sup> However, this work utilizes an order of magnitude less incident energy. With each measurement of energies averaged over 10 pulses, each optimization run requires  $\sim 5$  min. The limiting factor in execution speed is the 10 Hz repetition rate of the lasers. We were not able to experimentally determine the pulse shape (or equivalently, the relative phases of the seven incident sidebands) associated with any of the optimizations described in this paper.

In order to maximize or minimize the energy ratio of one sideband to another, we choose as our fitness function the ratio of integrated photodiode signals of the two sidebands in question. Figure 2 depicts four separate optimizations. Each optimization requires  $\sim 15$  min to complete and utilizes averaged values over 10 measurements, 10 pulse shapes per generation, and 15 generations. A total of 8.9 mJ of incident energy ( $\pm 10\%$  from pulse to pulse) is used with average energies of 0.74, 2.9, 1.7, 2.0, 0.96, 0.45, and 0.17 mJ for sidebands of wavelengths 1563, 1064, 807, 650, 544, 468, and 410 nm, respectively. Figures 2(a) and 2(b) show optimizations in which the energy of the 807 nm sideband changes by over 2 mJ and the energy of the 650 nm sideband changes by over 1 mJ between maximization and minimiza-

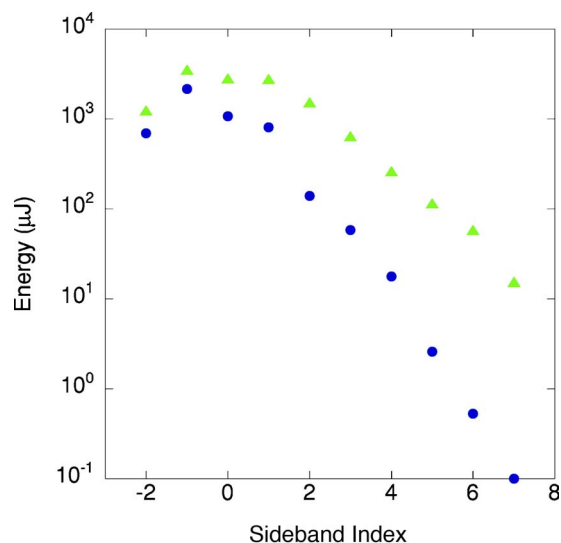


FIG. 4. (Color online) Control of sideband energy. The maximum (triangle) and minimum (circle) energies that can be generated for each sideband are depicted. The sidebands are labelled consecutively from  $-2$  ( $1.56 \mu\text{m}$ ) to  $7$  ( $300 \text{ nm}$ ) with the initial pump beams being  $-1$  ( $1064 \text{ nm}$ ) and  $0$  ( $807 \text{ nm}$ ).

tion. The energy ratio of the  $807 \text{ nm}$  sideband to the  $650 \text{ nm}$  sideband changes by a factor of 5. In contrast, Figs. 2(c) and 2(d) depict optimizations in which the energy ratio of the  $544 \text{ nm}$  sideband to the  $410 \text{ nm}$  sideband changes dramatically by a factor of 72 between minimization and maximization.

Figure 3 depicts the performance of the GA for the optimization of the ratio of  $544 \text{ nm}$  energy to  $410 \text{ nm}$  energy with each point being the average performance of a single generation of the GA. This graph represents typical GA convergence performance for the data presented in this paper. At the first generation, both maximization and minimization procedures begin with a similar average energy ratio as expected from random initial pulse shapes, but after a few generations they converge to sharply different average ratios.

Figure 4 is a representation of the maximum and minimum overall energies we can produce for each sideband. The data was generated by picking out the maximum and minimum energies for each sideband from the aggregate data

produced from the 1000 pulse shapes required to optimize energy ratios, as depicted in Fig. 2. The ratio of the maximum to minimum achievable energy at a wavelength is representative of our level of control over the energy of that wavelength. This energy ratio is 1.9, 2.1, 4.5, 7, 10, 11, 49, 100, and 150 for wavelengths of 1563, 1064, 807, 650, 544, 468, 410, 365, 329, and  $300 \text{ nm}$ , respectively.

In conclusion, we have shown limited control over multi-octave spectra using coherent control of molecular modulation. We have shown alteration of individual sideband energies by up to a factor of 150 as well as the efficient transfer of millijoules of energy from one color to another. It is likely that an extension of this work with an increase in the number of sidebands would result in greater control than presented here.

The authors thank Steve Harris for helpful discussions. This work was supported by the U.S. Air Force Office of Scientific Research and the U.S. Army Research Office.

<sup>1</sup>S. E. Harris and A. V. Sokolov, *Phys. Rev. A* **55**, R4019 (1997).

<sup>2</sup>A. V. Sokolov, M. Y. Shverdin, D. R. Walker, D. D. Yavuz, A. M. Burzo, G. Y. Yin, and S. E. Harris, *J. Mod. Opt.* **52**, 285 (2005).

<sup>3</sup>A. V. Sokolov, D. R. Walker, D. D. Yavuz, G. Y. Yin, and S. E. Harris, *Phys. Rev. Lett.* **85**, 562 (2000).

<sup>4</sup>D. D. Yavuz, D. R. Walker, G. Y. Yin, and S. E. Harris, *Opt. Lett.* **27**, 769 (2002).

<sup>5</sup>D. D. Yavuz, D. R. Walker, M. Y. Shverdin, G. Y. Yin, and S. E. Harris, *Phys. Rev. Lett.* **91**, 233602 (2003).

<sup>6</sup>S. Gundry, M. P. Anscombe, A. M. Abdulla, E. Sali, J. W. G. Tisch, P. Kinsler, G. H. C. New, and J. P. Marangos, *Opt. Lett.* **30**, 180 (2005).

<sup>7</sup>S. Sensarn, S. N. Goda, G. Y. Yin, and S. E. Harris, *Opt. Lett.* **31**, 2836 (2006).

<sup>8</sup>A. V. Sokolov, D. D. Yavuz, D. R. Walker, G. Y. Yin, and S. E. Harris, *Phys. Rev. A* **63**, 051801 (2001).

<sup>9</sup>R. Bartels, S. Backus, E. Zeek, L. Misoguti, G. Vdovin, I. P. Christov, M. M. Murnane, and H. C. Kapteyn, *Nature (London)* **406**, 164 (2000).

<sup>10</sup>B. J. Pearson and P. H. Bucksbaum, *Phys. Rev. Lett.* **92**, 243003 (2004); B. J. Pearson and P. H. Bucksbaum, *ibid.* **94**, 209901 (2005); M. Spanner and P. Brumer, *Phys. Rev. A* **73**, 023810 (2006).

<sup>11</sup>M. Y. Shverdin, S. N. Goda, G. Y. Yin, and S. E. Harris, *Opt. Lett.* **31**, 2836 (2006).

<sup>12</sup>M. Y. Shverdin, D. R. Walker, D. D. Yavuz, G. Y. Yin, and S. E. Harris, *Phys. Rev. Lett.* **94**, 033904 (2005).

<sup>13</sup>J. J. Grefenstette, <ftp://www.aic.nrl.navy.mil/pub/galist/source-code/ga-source>, 1995.